



**HAL**  
open science

# Impurity transport and its modification by MHD in tokamak plasmas, with application to tungsten in WEST

P. Maget, J Frank, O. Agullo, X. Garbet, H. Lütjens

## ► To cite this version:

P. Maget, J Frank, O. Agullo, X. Garbet, H. Lütjens. Impurity transport and its modification by MHD in tokamak plasmas, with application to tungsten in WEST. EPS 2019 - 46th European Physical Society Conference on Plasma Physics, Jul 2019, Milan, Italy. cea-02555124

**HAL Id: cea-02555124**

**<https://cea.hal.science/cea-02555124>**

Submitted on 27 Apr 2020

**HAL** is a multi-disciplinary open access archive for the deposit and dissemination of scientific research documents, whether they are published or not. The documents may come from teaching and research institutions in France or abroad, or from public or private research centers.

L'archive ouverte pluridisciplinaire **HAL**, est destinée au dépôt et à la diffusion de documents scientifiques de niveau recherche, publiés ou non, émanant des établissements d'enseignement et de recherche français ou étrangers, des laboratoires publics ou privés.

P. Maget<sup>1</sup>, J. Frank<sup>1,2</sup>, O. Agullo<sup>2</sup>, X. Garbet<sup>1</sup>, H. Lütjens<sup>3</sup>, and the WEST team<sup>4</sup>

<sup>1</sup> CEA, IRFM, F-13108 Saint Paul-lez-Durance, France.

<sup>2</sup> Aix-Marseille Université, CNRS, PIIM UMR 7345, 13397 Marseille Cedex 20, France.

<sup>3</sup> Centre de Physique Théorique, Ecole Polytechnique, CNRS, 91128 Palaiseau, France.

<sup>4</sup> see <http://west.cea.fr/WESTteam>

West

## Summary

- Neoclassical impurity transport & poloidal asymmetry
  - Can be determined analytically in a self-consistent way
  - Natural asymmetry (no torque) has already a large impact
- A magnetic island suppresses thermal screening above a critical size
  - Verified numerically on a typical WEST plasma equilibrium
- When impurity transport is predominantly turbulent (as on WEST)
  - Poloidal asymmetry remains essentially neoclassical

## Neoclassical impurity transport & self-consistent poloidal asymmetry

### Neoclassical impurity transport

- With a poloidal distribution parametrized as  $n_a/\langle n_a \rangle = 1 + \delta \cos \theta + \Delta \sin \theta$  [1]:

$$\langle \Gamma_a \cdot \nabla r \rangle \approx -\langle n_a \rangle D_{PS}^a \left[ \left( 1 + \frac{\delta}{\varepsilon} + \frac{\delta^2 + \Delta^2}{4\varepsilon^2} \right) G + \frac{1}{2} \left( \frac{\delta}{\varepsilon} + \frac{\delta^2 + \Delta^2}{2\varepsilon^2} \right) U \right]$$

- with  $D_{PS}^a \equiv 2q^2 m_a \nu_a T_a / (e_a^2 \langle B^2 \rangle)$ ,  $C_0 \sim 1.5$  and  $k_i \sim 1, 17$  in the banana regime

$$G = \partial_r \ln p_a - \frac{e_a T_i}{e_i T_a} \partial_r \ln p_i + C_0^a \frac{e_a T_i}{e_i T_a} \partial_r \ln T_i \quad U \approx - (C_0^a + k_i) \frac{e_a T_i}{e_i T_a} \partial_r \ln T_i$$

### Poloidal asymmetry

- Asymmetry parameters  $(\delta, \Delta)$  verify:

$$\Delta^2 + (\delta - C_\delta)^2 = R_\Delta^2$$

- with  $C_\delta = -\varepsilon / (1 + U/G)$ ,  $\varepsilon = r/R$ , and  $R_\Delta = |C_\delta|$

- Defining  $\delta = C_\delta + R_\Delta \cos \alpha$  and  $\Delta = R_\Delta \sin \alpha$

$$\cos \alpha = \frac{R_\Delta (AG\varepsilon)^2 - R_\Delta^2}{C_\delta (AG\varepsilon)^2 + R_\Delta^2}, \quad \sin \alpha = 2R_\Delta \frac{AG\varepsilon}{(AG\varepsilon)^2 + R_\Delta^2}$$

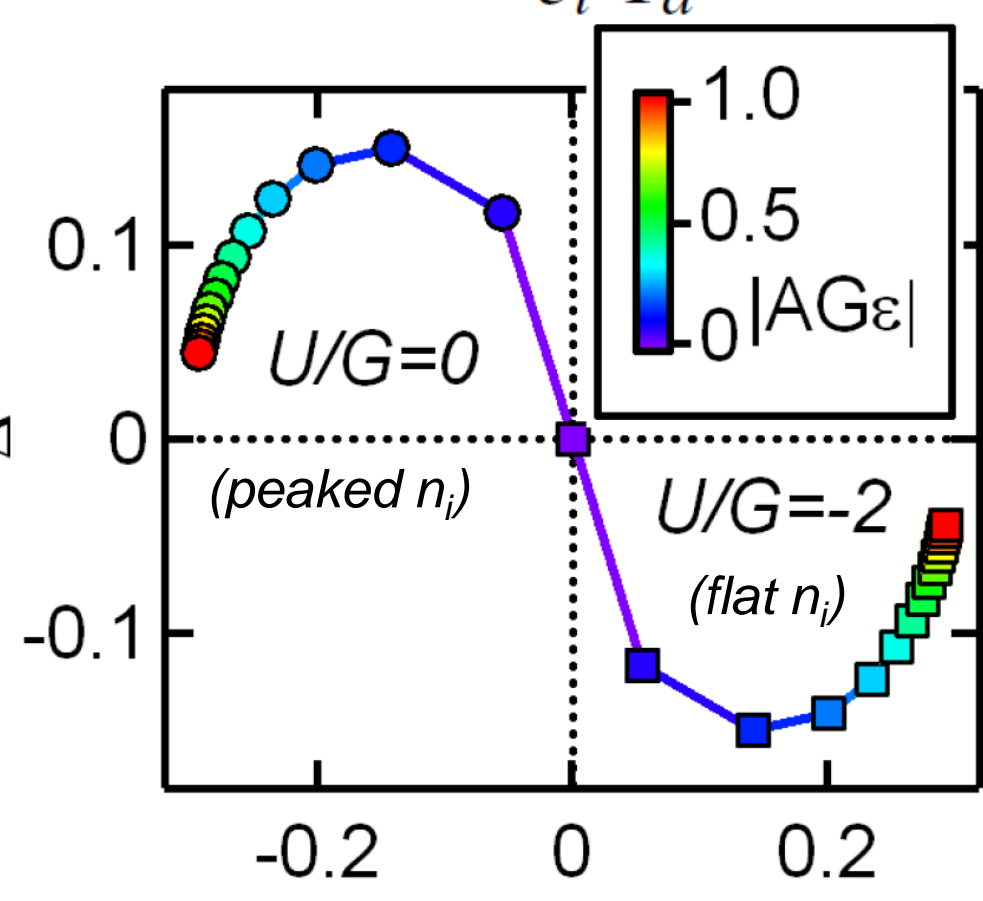
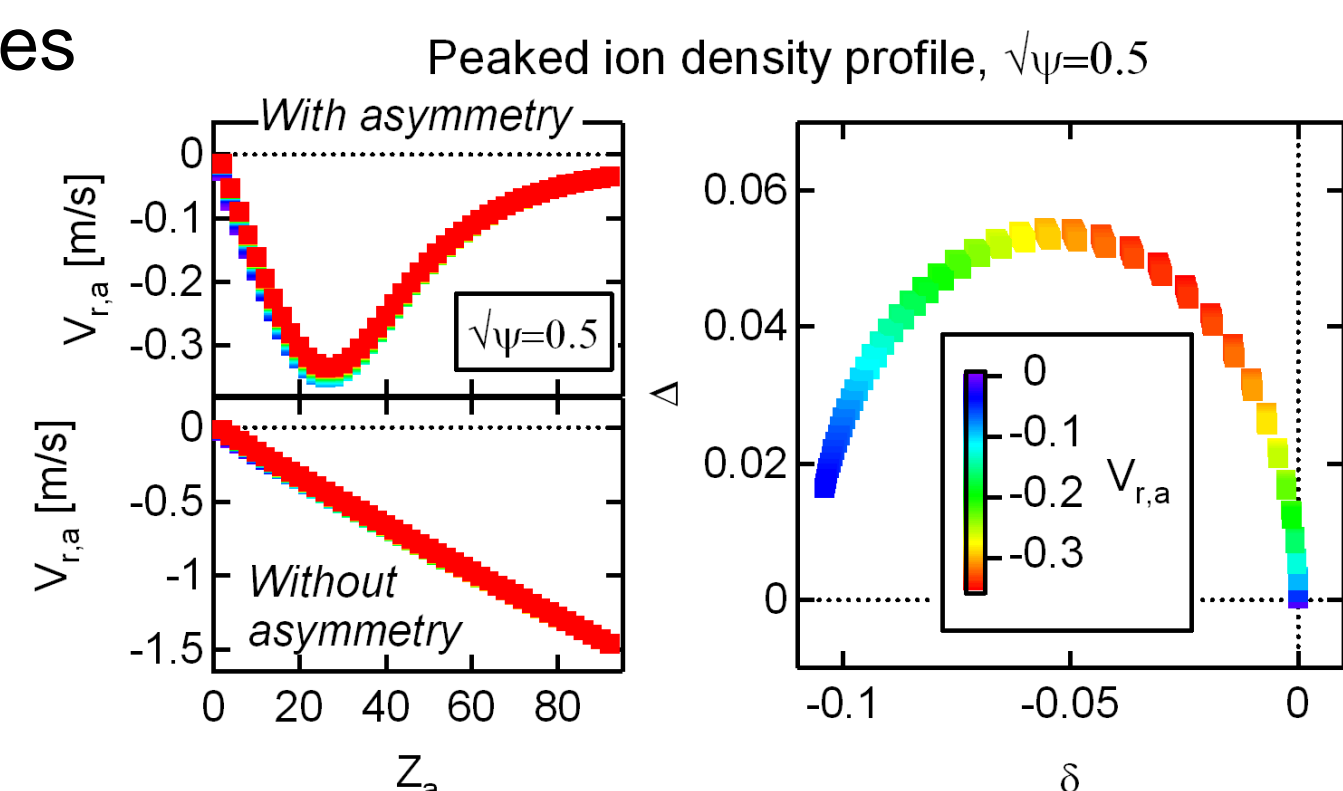


Fig. 1 : Self-consistent asymmetry

- This fully determines the self-consistent asymmetry when the ion and electric potential asymmetries can be neglected (the formula can be extended in these cases).
- Characteristics of the asymmetry circle (fig. 1 & 2)
  - The circle is centered at  $\delta < 0$  for a peaked ion density profile ( $\delta > 0$  for a flat one)
  - The asymmetry angle  $\alpha$  increases with impurity charge  $[A = q^2 R \nu_a / (\varepsilon^2 \Omega_a) \sim Z_a]$
- At saturation ( $V_{r,a} = 0$ ), the asymmetry vanishes

Fig.2 : Radial impurity flow as a function of the impurity charge  $Z_a$  with & without self-consistent poloidal asymmetry (left); corresponding asymmetry (right). The impurity profile is flat.



## Neoclassical impurity transport: numerical settings

Numerical experiments are performed with the XTOR-2F code [2] including neoclassical physics [3] and two equations per impurity:

$$\partial_t n_a + \nabla \cdot (n_a \mathbf{V}_a) = -\nabla \cdot \Gamma_a^{turb}$$

$$m_a n_a D_t V_{a||} = -\nabla_{||} p_a + n_a e_a E_{||} + R_{a||} - (\nabla \cdot \Pi_a)_{||}$$

with  $\frac{R_{a||} - (\nabla \cdot \Pi_a)_{||}}{m_a n_a} = \nu_a \left( V_{i||} - V_{a||} - C_0^a \frac{2q_i}{5p_i} \right) + \dots$  (small terms)

- The impurity-ion collision frequency  $\nu_a$  is scanned artificially
- We consider a peaked and a flat ion density profile (same pressure) (fig.3a)
- Turbulent diffusion coefficient is set to a very low value (fig.3b)

Fig.3a : Ion density and temperature profiles.

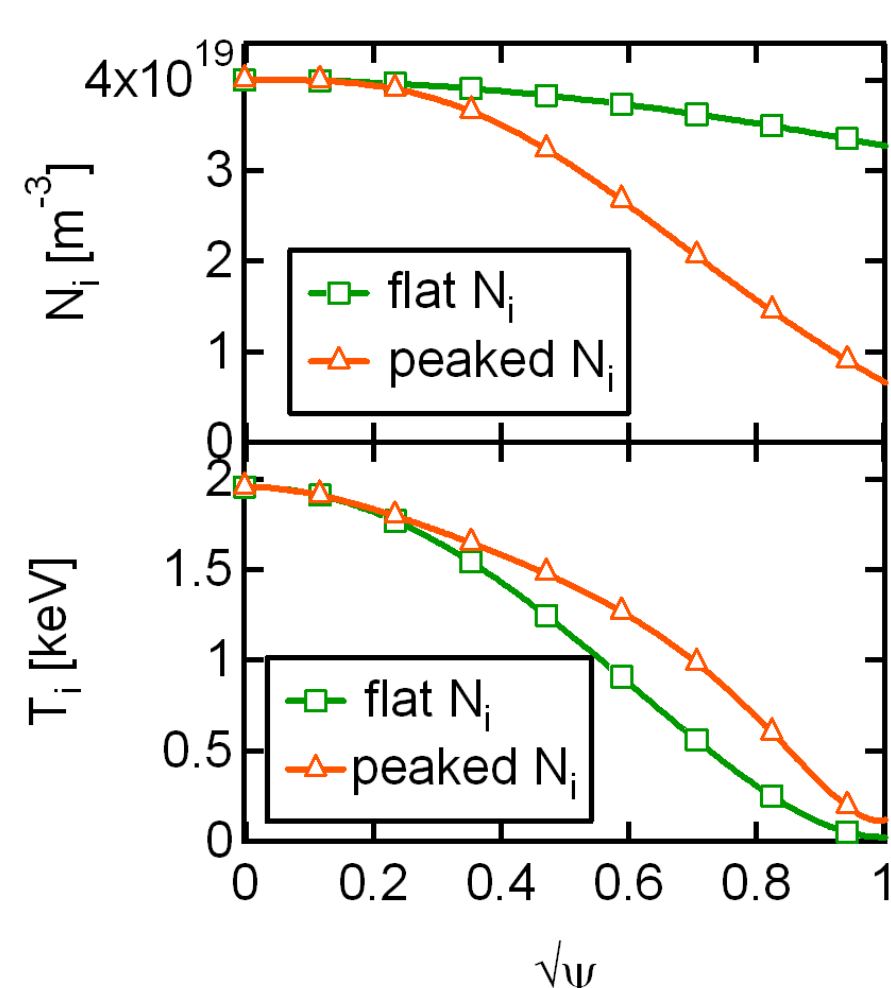
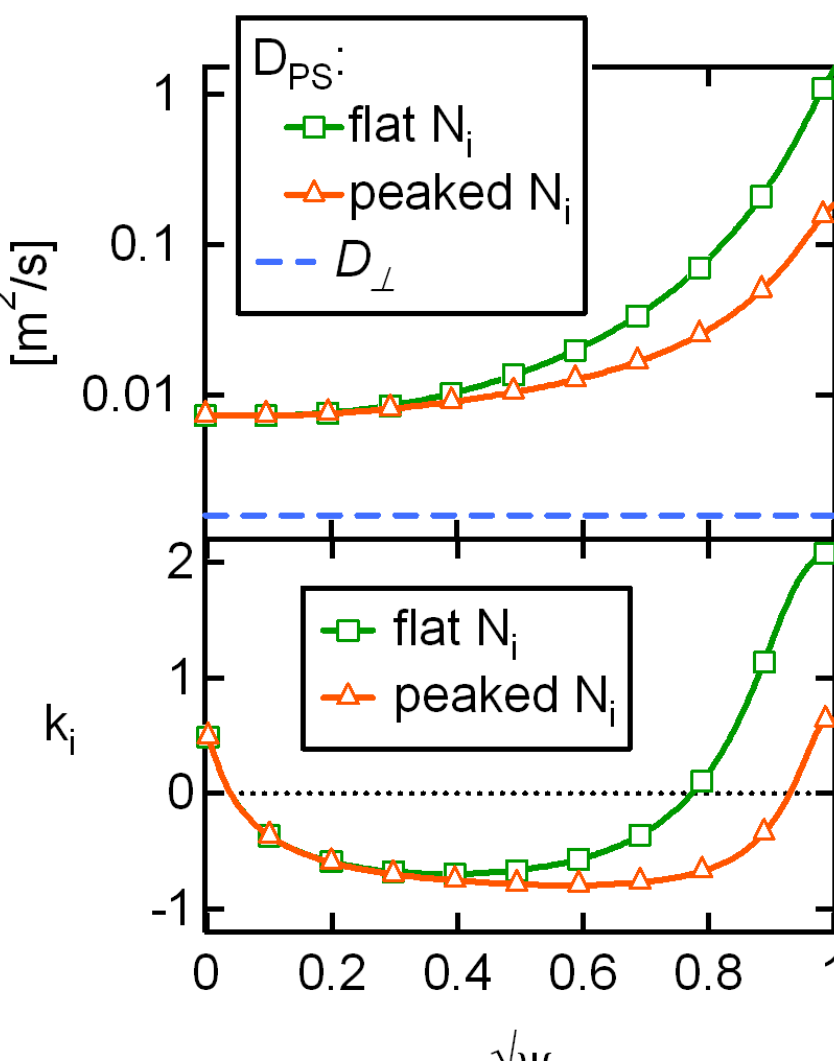


Fig.3b: Pfirsch-Schlüter diffusion coefficient &  $k_i$  parameter.



## References

- [1] Angioni et al *PPCF* **56** 124001 (2014)  
 [2] Lütjens *J. Comp. Phys.* **229** 8130 (2010).  
 [3] Maget *NF* **56** 086004 (2016); **59** 049501 (2019).  
 [4] Hender *Nuclear Fusion* **56** 066002 (2016).  
 [5] Fitzpatrick *Physics of Plasmas*, **2** 825 (1995).  
 [6] Bourdelle, *this conference* **O5.101**  
 [7] Yang, *this conference* **P5.1085**

## Neoclassical impurity transport: validation

### Impurity flow & poloidal asymmetry during the (artificial) collisionality scan

- Impurity : Tungsten  $W^{44+}$ , flat initial profile, and decreasing collisionality (fig.4)

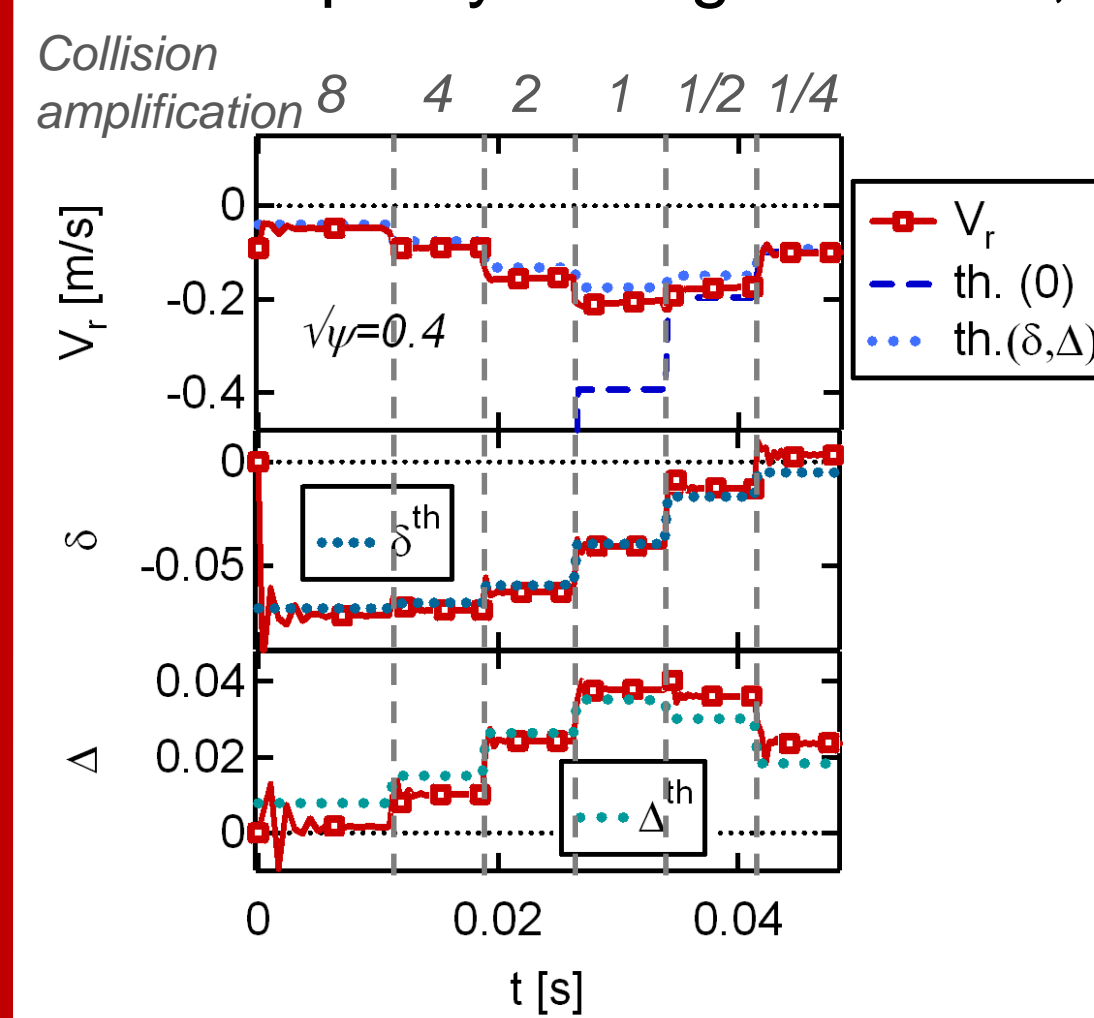


Fig.4 : Radial flow,  $\delta$  and  $\Delta$  during the collisionality scan with factor 8, 4, 2, 1, 0.5, 0.25 (peaked ion density profile).

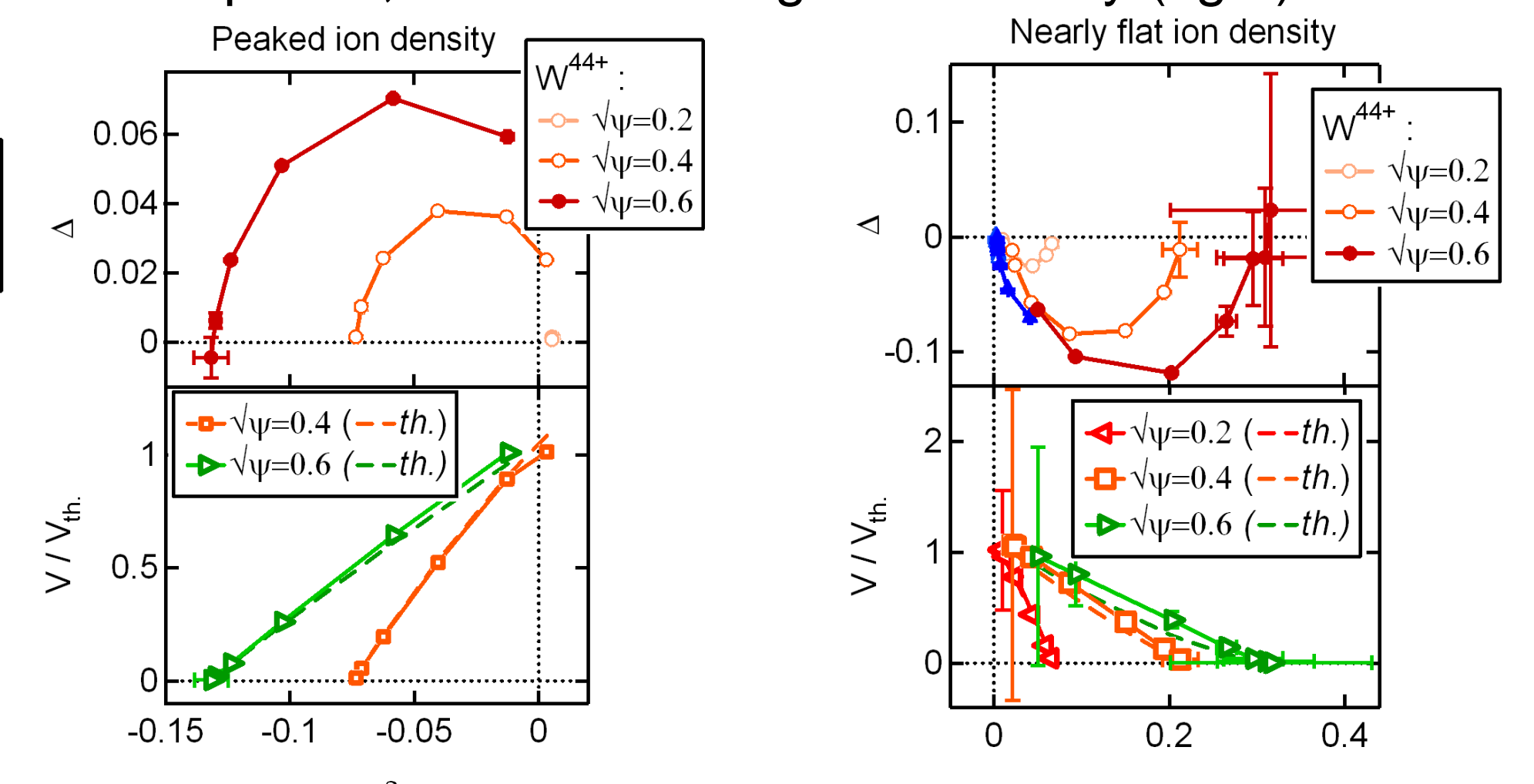
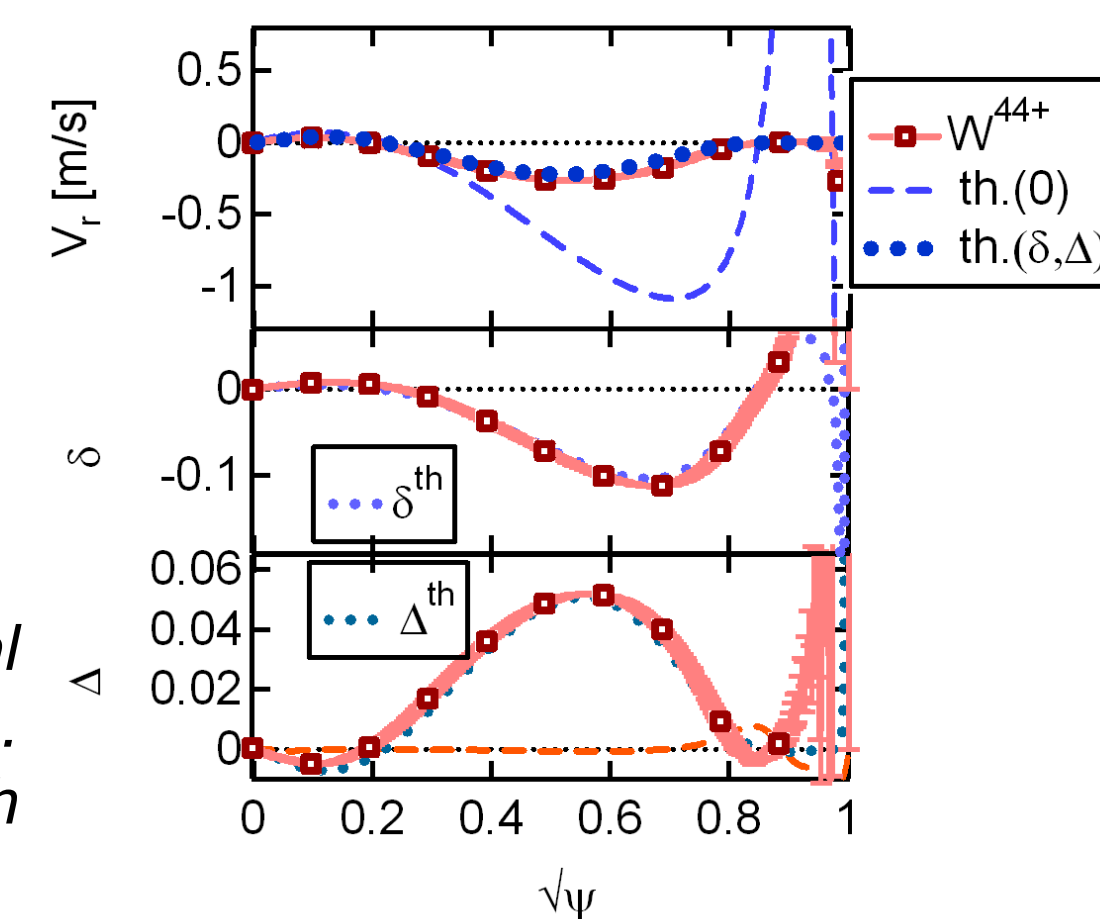


Fig.5 : Asymmetry (top) and ratio of radial flow to theoretical value without asymmetry (bottom), for the peaked and flat ion density profiles, and several radial positions.

### Radial flow & poloidal asymmetry vs theoretical model

- The asymmetry circle is reproduced (fig. 5)
- The radial flow & poloidal asymmetry profiles are well predicted (fig.6).
- Radial  $W^{44+}$  flow is damped for both the peaked & flat ion density profiles (fig.5 & 6)

Fig.6 : Radial flow,  $\delta$  and  $\Delta$  profiles for the real collisionality (peaked ion density profile). Comparison of simulation results with theory with  $(th(\delta, \Delta))$  and without  $(th(0))$  poloidal asymmetry.



## Neoclassical impurity transport in presence of a (2,1) island on WEST

### Magnetic islands remove the outward thermal screening term

- This mechanism could accelerate plasma contamination [4]
- A (2,1) island is inserted in a WEST equilibrium and decays to  $W_{sat} \sim 4\%$  (fig.7)
- Locally, the radial flow of  $W^{28+}$  approaches its theoretical value without thermal screening (fig.8).

The radial flow can be fitted by a tanh by introducing the characteristic transport width  $W_\chi$  [5] (fig.9).

$$V_{r,W} = V_{r,W}^0 + V_{r,W}^{isl} \times [1 + \tanh 3 (W - 1.8W_\chi) / W_\chi]$$

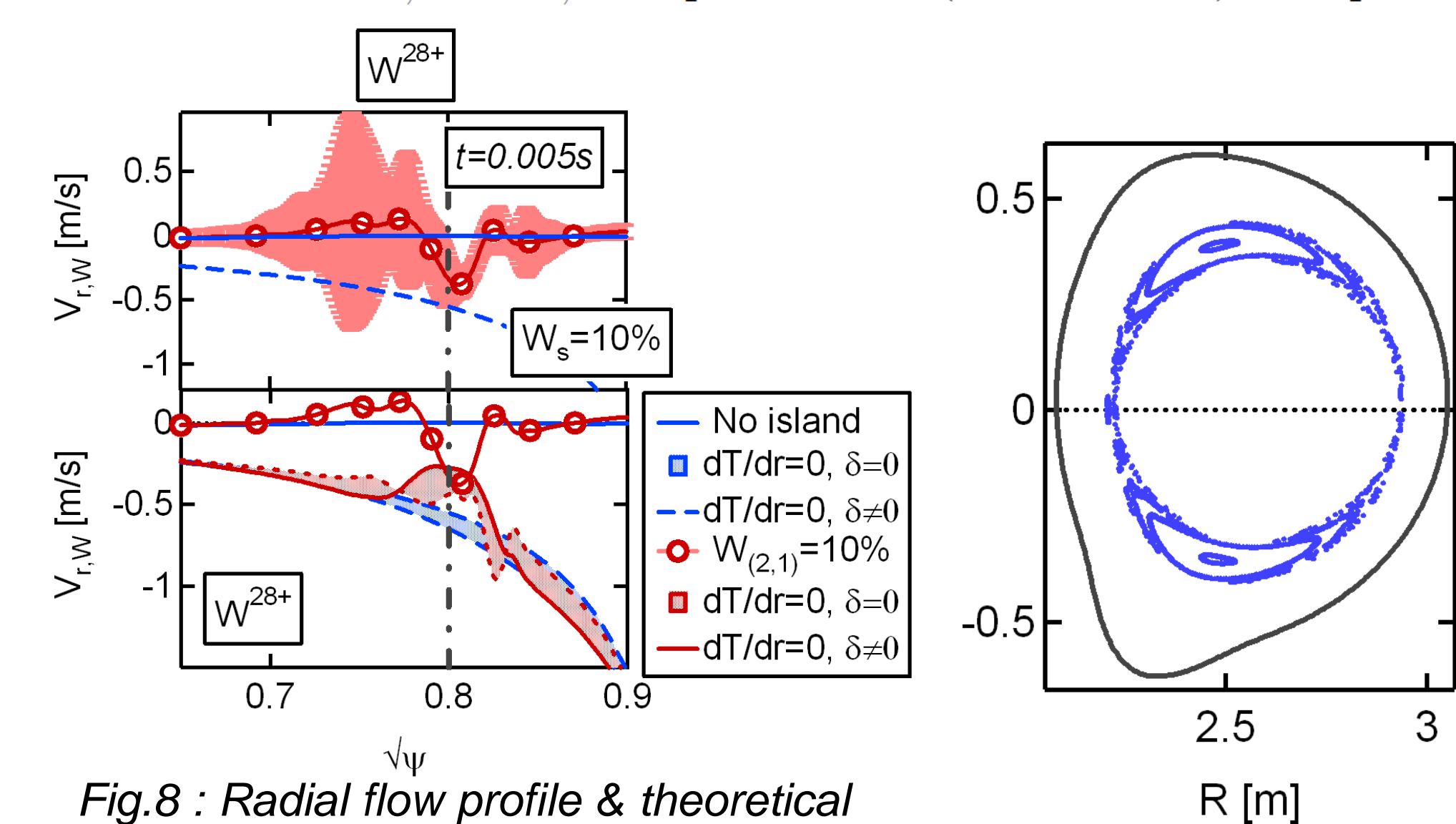


Fig.8 : Radial flow profile & theoretical flow without thermal screening

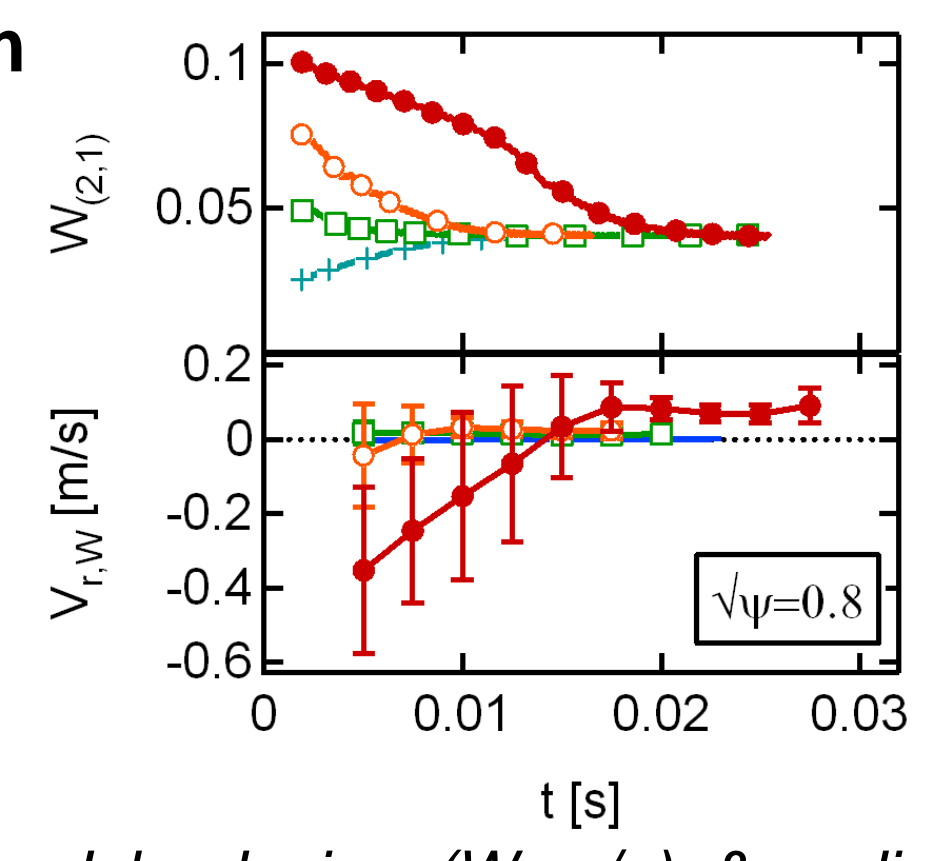


Fig.7 : Island size ( $W=w/a$ ) & radial flow at the island position for # seeds.

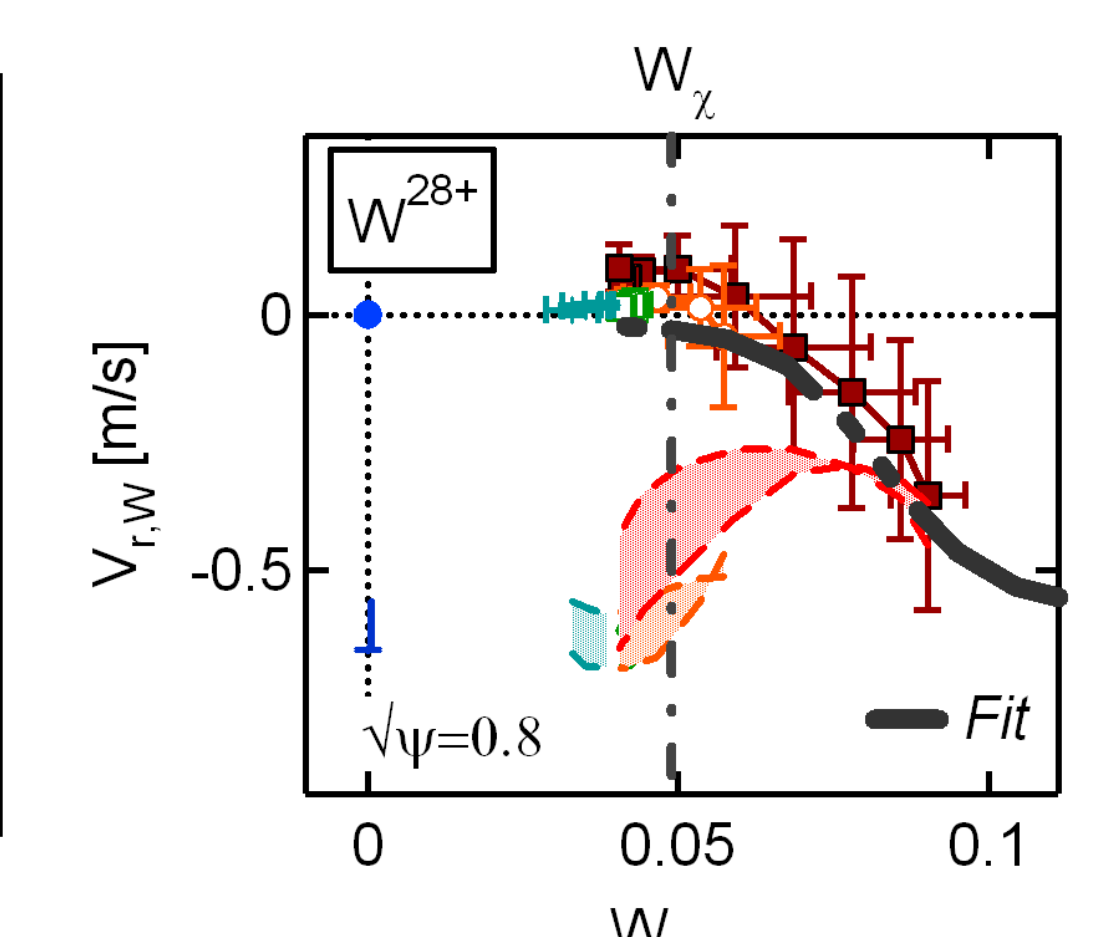


Fig.9 : Radial flow as a function of (2,1) island size.

## Turbulent impurity transport on WEST

### The Tungsten transport is in fact dominated by turbulence on WEST [6,7]

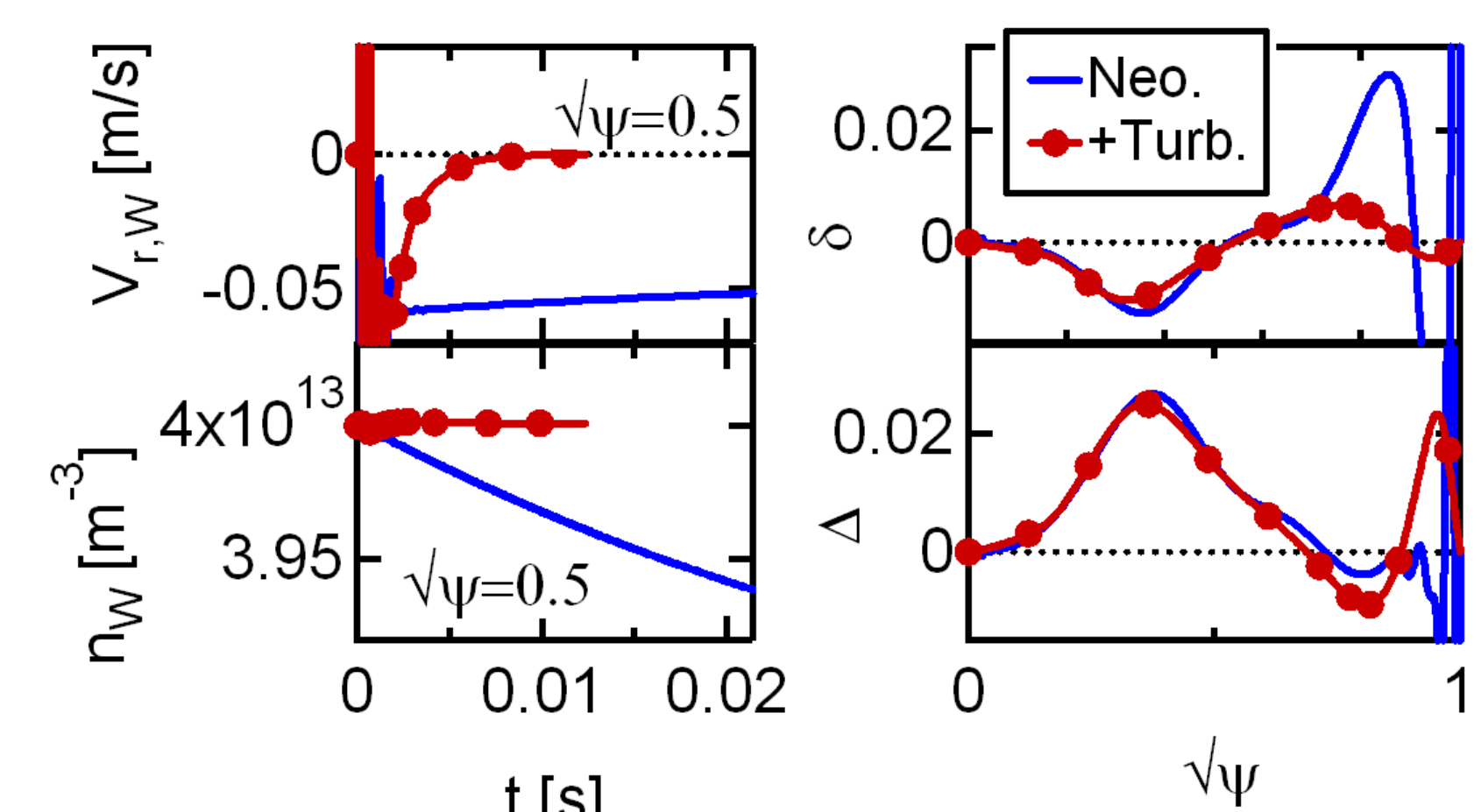
- An ad-hoc model is implemented in XTOR with  $D_{\perp} = 8m^2/s$ ,  $D_{thd} = 0.8m^2/s$ ,  $V_{cur} = -6.7m/s$ :

$$\Gamma_a^{turb} = -D_{\perp}^a \nabla n_a + n_a \mathbf{V}_p^a$$

$$\mathbf{V}_p^a = D_{thd}^a \nabla \ln T_a + \mathbf{V}_{cur}^a$$

- The Tungsten profile remains flat as observed experimentally [7]
- Poloidal asymmetry remains close to its neoclassical value (fig.10).

Fig.10 : Radial flow &  $W^{28+}$  density at  $\nu_{\psi} = 0.5$  (left); asymmetry profiles with and without turbulence (right).



## Acknowledgements

Work carried out within the framework of the FR-FCM & EUROfusion Consortium ; funding from the Euratom research and training programme 2019-2020 (grant 633053, project ENR-MFE19.CEA-03). The views and opinions expressed herein do not necessarily reflect those of the European Commission.

Numerical resources provided by GENCI (project 056348), Mésocentre of Aix-Marseille University (project b009), MARCONI-EUROfusion (project NISMO)